

A New Trade-off Scheme for MIMO OFDM-based Cognitive Radio Systems over Correlated Fading Channels

Makan Zamanipour

IEEE Member

Tehran, Iran

Makan.zamanipour.2015@ieee.org

Saeed Mashhadi

Sharif University of Technology

Tehran, Iran

mashhadi@sharif.edu

Abstract—A joint pre- and post-coder (JPROC) is proposed for MIMO OFDM-based cognitive radio systems over correlated fading channels. The main aim is to have a trade-off between licensed networks and un-licensed networks in the *underlay scenario*. To handle the un-desired interferences on the main networks, the eigen-values of this JPROC should be small in each licensed network, as much as possible, whereas un-licensed users have higher rates. Frequency selective MIMO fading channels are coded with orthogonal space-time-frequency block codes (OSTFBCs) to improve the bad effects of these small eigen-values on the signal to noise ratio (SNR) in the main network. On the other hand, the system is operated in both transmit- and receive-correlation scenarios. We have the correlation matrices at all the transmitters imperfectly. This is because there is any error in the estimation of the transmit- and the receive- *angle spreads*. The matrix of the JPROC is obtained by solving a robust convex optimization problem in the multi-user scenario. The optimization problem is represented under some constraints such as the outage probability of eavesdropping as a criterion for secrecy. An upper-band of the pair-wise error probability is minimized, while controlling the produced interferences. The effective performance of this JPROC is finally shown using simulations.

I. INTRODUCTION

The emerging technologies play as a key role in gaining telecommunications systems. These emerging technologies have been done for cognitive radio systems as next-generation wireless communications. In the *underlay scenario*, two kinds of users are supposed to be serviced well, namely *primary* users (PUs) as licensed users and *secondary* users (SUs) as un-licensed users.

Motivations are given as follows. Pre-coding and JPROC have been proposed for MIMO systems e.g. by [2-4] due to their ability to combat the correlation effects of spatially correlated channels. Recently, it has been extended for MIMO OFDM-based cognitive radio systems e.g. by [1]. Indeed, while MIMO fading channels are more correlated, the condition numbers of correlation matrices

are correspondingly increased. In other words, the eigen-values of correlation matrices are revealed in the denominator of the pair-wise error probability. Therefore, the eigen-values of the pre-coder/JPROC matrix can handle the smaller eigen-values under some constraints that are described as follows.

An overview of methodologies and justifications is given as follows. The main aspect of our study is to establish a new secure and acceptable trade-off scheme for the mentioned systems. Indeed, we aim to design respectively a JPROC at each PU transmitter and PU receiver with respect to a trade-off between SU and PU networks in order to service all of them efficiently. Indeed, JPROC is jointly a pre-coder at the main PU transmitter and a post-coder at the main PU receiver. In this work, the eigen-values of the JPROC matrix are supposed to be very small, as much as possible. Based on this point, in the *underlay scenario*, the produced interferences by SU networks and other PU networks on the considered PU network can be controlled, whereas SUs can have higher rates. Although these small eigen-values make reduction in SNR in the main network, but the important interference power constraint related to the considered PU network is satisfied very well. On the other hand, the quality of service of the considered PU network as the probability of error should be improved. This is guaranteed by applying OSTFBCs, *without loss of generality*. This is guaranteed due to the ability of OSTFBCs to increase the diversity order based on the frequency domain as third domain.

An *important question* is why no pre-coder with the very small eigen-values is designed at each SU transmitter. This is because the transmit-power at the SU transmitters are not supposed to be decreased, while all the interferences that are caused by SUs (and other PUs) should be controlled in the *underlay scenario*. In other words, as a trade-off between PU networks and SU networks, SUs have higher rates. Meanwhile, secrecy as the low outage probability of eavesdropping need to be guaranteed in this

scheme. Indeed, secrecy is a very important criterion, whereas the mentioned trade-off is supposed to be performed. Secrecy for cognitive radio systems has been investigated e.g. by [9, 20].

Our contributions are given as follows. The main topic as the trade-off scheme is the main contribution. On the one hand, unconventionally, the eigen-values of the JPROC matrix are supposed to be very small, as much as possible. In the underlay scenario, this makes to control the interferences, whereas SUs can have higher rates. On the other hand, unlike previous works, OSTFBCs are used for MIMO OFDM-based cognitive radio systems in frequency selective correlated Rayleigh fading channels. The mentioned work has not been investigated for these systems until now. The method of the ST/SF Coding was completely explained e.g. by [14-15], whereas we extended that to the mentioned systems as emerging technologies. The other contributions are actualized as follows.

The third contribution is discussed as follows. The outage probability of eavesdropping (as secrecy) has not been considered as a constraint in the pre-coded MIMO OFDM-based cognitive radio systems over correlated fading channels until now. This topic is examined as a criterion in this work unlike previous studies. On the other hand, as pointed out before, there is no conflict between secrecy and cognitive schemes. Secrecy for multi-user cognitive radio systems has been investigated e.g. by [20].

The other difference between pervious works (such as [1, 5]) and this research is that the mentioned system is operated in the multi-user scenario. Consequently, this makes that the used optimization problem is generalized to different one, without loss of generality. This work compared to e.g. [19-21] is more comprehensive, having more complicated equations.

Meanwhile, robust beam-forming has been widely explored for OSTB Coded MIMO-based cognitive radio systems under the imperfect channel state information (CSI) at the transmitter e.g. by [5-13]. The paper extends that for OSTFB Coded MIMO OFDM-based cognitive radio systems, considering a novelty. Since an optimization problem is not convex when a parameter is not known such as channels or angle spreads, this needs to be robustly solved as a *relaxation method*. The related design problems have been robustly considered in [5-13] with imperfect CSI at the transmitter, whereas the study extends that more in details.

Similar works have been widely investigated for MIMO OFDM-based cognitive radio systems (such as [1], or such as [5] in the single-carrier scheme). It can easily be noted that less attention has been given in previous works for

design of a pre-coder/JPROC for these systems. Furthermore, additional criteria need to be considered. In this work, the error rate, the interference power and the secrecy are jointly considered. These criteria are considered in more real conditions such as frequency selective fading channels. Moreover, the comprehensive integration of the mentioned technologies are used to further improve the system performance in this study.

One important disadvantage of the proposed scheme is discussed as follows. The convergence in the simulations is guaranteed, but it is well-known that the convergence time is slow because of the complexity of the system. Nevertheless, the complexity of the system is quantified in terms of running time using *tic-toc* in MATLAB.

The paper is organized as follows. At first we present the multi-user network, the data-applying in the used OSTFB Coded MIMO-OFDM scheme over frequency selective channels, system model and the equations of the used correlated channels in Section II. The robust JPROC design problem is formulated for the mentioned systems in Section III, when operating in both transmit- and receive-correlation scenarios [1-Sec. IV-A]. Performance checkout as closed-form solution is stated in Section IV. The analytical results in order to prove the effective performance of the mentioned JPROC are presented in Section V. Conclusions are given in Section VI, and proofs and more discussions are stated in the Appendix at the end of this paper.

In this paper, $P_l P_l$ in $(.)_{P_l P_l}$ refers to the l th PU transmission to the l th PU receiver as the main link (channel) for the main network. $\delta(.)$ is the derivative operation. \mathbf{I}_n represents the n -by- n identity matrix. $\mathbf{\Lambda}$ refers to eigen-value matrices and λ refers to an eigen-values. Some of the useful notations that are used throughout the paper are listed in Table I.

TABLE I. NOTATIONS

Notation	Definition
Boldfaced Upper-Case Character \mathbf{A}	Matrix
Boldfaced Lower-Case Character \mathbf{a}	Vector
Non-Boldfaced Lower -Case Character a	Scalar
(1)	Equation (1)
(k)	k th Sub-carrier
Number of sub-carriers	K
(l)	l th (S/P) User
Number of Users	L
$(.)^H$	Hermitian
$\ .\ _F$	Frobenius Norm
$Tr(.)$	Trace of a matrix
$(.)^*$	Conjugate
$(.)^{1/2}$	Square Root

II. SYSTEM DESCRIPTION

A. Network description

The basis of the considered cognitive radio system is that the mentioned linear JPROC is achieved based on solving a robust convex optimization problem. The convexity of this problem is proven. Design at transmitters in every system is cheaper than receivers. So, this analysis is represented at each PU transmitter and the acquired values are reported by using any feedback to the related receiver. Note that undoubtedly, this JPROC can affect in the norm of the equivalent channels, because this is linear. Note that *equivalent channel* throughout the paper refers to this point.

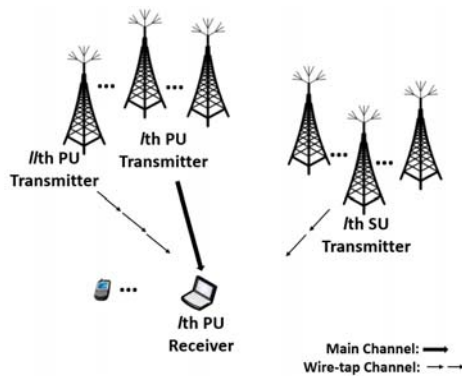


Fig. 1. Cognitive radio network

A cognitive radio network is depicted in Fig.1. L PUs coexist very well with L SUs based on the underlay scenario. All PUs and SUs are equipped with $N_t \times N_r$ transmit-receive-antennas. The main channel is depicted as boldfaced arrows, whereas the wire-tap channels are shown as dotted arrows. Meanwhile, secrecy for the main network is defined related to SU networks. See Section III for more discussion. Since secrecy is a criterion, *wire-tape channel* definition is considered.

B. Frequency selective channels

In this part, the used frequency selective fading channels are described. Consider D *delay taps* for each element of the mentioned MIMO channel matrices. Meanwhile, consider uniform power delay profile for these taps in time domain. The condition $\delta_d^2 = 1/D$ is satisfied for channel normalization. These variances weight the channel indices. It is well-known that normally the delays of these taps as time delay groups are considered equally for flat fading channels. Now, by knowing that the number of the used sub-carriers (and the used *cyclic prefix*) is enough for D delay taps, the inter-channel interferences can be neglected. Now, the sub-channels are flat. Let us explain it more. The difference between flat and frequency selective fading channels is applied as follows. The fading amplitudes

versus frequency are constant in flat mode, whereas they are variable in frequency selective mode. The correlation matrices are considered like that. This is because of the possibility of deletion of directions (paths) in frequency selective fading channels. This refers to the random parameter *angle spread* (spreading in *angle of departure* at transmitters or in *angle of arrival* at receivers) which was discussed in [1]. For example, the sub-channel matrix $H(k)$ for the k th sub-carrier versus frequency is different from $H(k')$, $k' \neq k$. Now, it can be said that the channel indices are obtained by taking any average on the mentioned weighted taps and we consider this average. t is used for this average that is satisfied in all the equations in frequency domain. In addition, with respect to that the sub-channels are different, we can have the frequency diversity.

In general, a frequency selective channel in time domain can be implied as [15, 22]:

$$h_{a,b}(\vartheta) = \sum_{d=1}^D \alpha_{a,b}(d) \delta(\vartheta - \vartheta_d), \quad (1)$$

where ϑ_d is the time delay of the d th path and $\alpha_{a,b}(d)$ is the fading amplitude in the d th path between the a th transmit-antenna and the b th receive-antenna. In frequency domain, with respect to *Dirac delta* terms $\delta(\vartheta - \vartheta_d)$, applying fast Fourier transform on (1) makes to have phases:

$$H(k) = \sum_{\vartheta=1}^D h_{a,b}^k(\vartheta) e^{-j2\pi\vartheta k/K}. \quad (2)$$

These phases have no effect on autocorrelation matrices as covariance matrices. The k th sub-channel in frequency domain can be written as (2).

C. OSTFB coding

In this part, the method of OSTFB Coding based on the data applying is described. As an example, a 2×2 transmit-receive antenna is assumed in Fig.2. Meanwhile, there are 4 sub-carriers for simplicity. For instance, C_1 and $C_1(1)$ stand for a high rate data stream and its first sub-data, respectively. Each sub-data is applied on the related sub-channel which tuned on the related sub-carrier (under the assumption that BPSK modulation is used which can be generalized to the others).

As illustrated in Fig.2, each sub-data matrix is coded in the next neighbor frequency selective sub-channel again. It should be noted that now, all the available domains can be used for diversity, i.e., the antennas, the times and the sub-carriers. In this study (based on Fig.2), half of the sub-carriers are used for spatial multiplexing. This makes that the diversity gain is multiplied by at most 2 compared to that all of them are used for spatial multiplexing. This

refers to the frequency diversity. See the Appendix for more discussion. This term is neglected in all the related equations for more simplicity. How to detect the received sub-datas is given as follows.

		1th Receiver (1th Time Slot)		2th Receiver	
1th Transmitter	1th Sub-channel	$C_1(1)$	$C_2(1)$	$C_2(1)$	
	2th Sub-channel	$-C_2(1)^*$	$C_1(1)^*$	$C_1(1)^*$	
	3th Sub-channel	$C_1(2)$	$C_2(2)$	$C_2(2)$	
	4th Sub-channel	$-C_2(2)^*$	$C_1(2)^*$	$C_1(2)^*$	
2th Transmitter	1th Sub-channel	$-C_2(1)^*$	$C_1(1)^*$	$C_1(1)^*$	
	2th Sub-channel	$C_1(1)$	$C_2(1)$	$C_2(1)$	
	3th Sub-channel	$-C_2(2)^*$	$C_1(2)^*$	$C_1(2)^*$	
	4th Sub-channel	$C_1(2)$	$C_2(2)$	$C_2(2)$	

Fig.2. The method of OSTFB Coding based on the data applying

D. System model

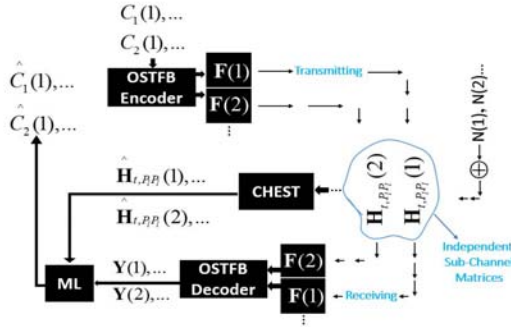


Fig.3. System model

As declared in Fig.3, at first, for the mentioned PU network, the l th sub-datas of C_1 and C_2 as bits are applied to OSTFB encoder (under the assumption that BPSK modulation is used). They are OSTFB encoded as described in the pervious part. Then, they are pre-coded by $\mathbf{F}(1)$ and $\mathbf{F}(2)$ of sizes $N_t \times N_t$ at the transmitter in the l th and the 2th sub-carriers, respectively. After transmitting over the independent sub-channel matrices $\mathbf{H}_{t,P_l}(1)$ and $\mathbf{H}_{t,P_l}(2)$, they are post-coded by $\mathbf{F}(1)$ and $\mathbf{F}(2)$ of sizes $N_r \times N_r$ at the receiver in the l th and the 2th sub-carriers, respectively (under the assumption that $N_t = N_r$). Then, they are OSTFB decoded. Finally, ML as the maximum likelihood detector recovers the received sub-datas. This is fulfilled with respect to CHEST as CHannel ESTimator. How to detect the received sub-datas (the elements of the matrix $\mathbf{Y}(1)$ in Fig.3) is given in Appendix A.

In Fig.3, $\hat{\cdot}$ indicates the estimation operation. $\mathbf{H}_{t,P_l}(1)$ and $\mathbf{Y}(1)$ indicate the first sub-channel matrix and the first received sub-data matrix in the l th sub-carrier,

respectively. The noise matrices that equally have the variance σ_n^2 for all the sub-channels, are considered in each $\mathbf{Y}(k)$ as $\mathbf{Y}(k) = \mathbf{F}(k)\mathbf{H}_{t,P_l}(k)\mathbf{F}(k)\mathbf{C}_i(k) + \mathbf{N}(k)$. As illustrated in Fig.3, these matrices are applied for the l th and 2th sub-channel matrices.

E. The equations of the used correlated channels

Based on the Kronecker model, the model of the considered frequency selective correlated Rayleigh fading channels for the k th sub-carrier related to the l th PU receiver can be written as:

$$\mathbf{H}_{t,P_l}(k) = \mathbf{R}_{t,P_l}^{1/2}(k)\mathbf{H}_{w,t,P_l}(k)\mathbf{T}_{t,P_l}^{1/2}(k), \quad (3)$$

$$\mathbf{H}_{t,P_l}(k) = \mathbf{R}_{t,P_l}^{1/2}(k)\mathbf{H}_{w,t,P_l}(k)\mathbf{T}_{t,P_l}^{1/2}(k), \quad (4)$$

$$\mathbf{H}_{t,S_l}(k) = \mathbf{R}_{t,S_l}^{1/2}(k)\mathbf{H}_{w,t,S_l}(k)\mathbf{T}_{t,S_l}^{1/2}(k). \quad (5)$$

For example, in (5), \mathbf{T}_{t,S_l} and \mathbf{R}_{t,S_l} are respectively the transmit- and the receive-correlation matrices of sizes $N_t \times N_t$ and $N_r \times N_r$ related to the channel between the l th SU transmitter and the l th PU receiver (\mathbf{H}_{t,S_l}). For example, (4) implies the channel between the l th PU transmitter and the l th PU receiver. The matrices \mathbf{H}_{w,t,P_l} , \mathbf{H}_{w,t,S_l} and \mathbf{H}_{w,t,P_l} of sizes $N_r \times N_t$ as white channel matrices, have independent and identically distributed zero-mean and unit-variance circular symmetric complex Gaussian elements. As discussed in II-B, t is used for the averaged frequency selective channels.

III. DESIGN PROBLEM FORMULATION

The main challenge is to keep the quality of service for each PU, whereas SUs are extraordinary serviced based on the underlay scenario with higher rates. Higher rates for SUs refer to Q that will be described in 8th equation. In this design the quality of service is considered as the low probability of error.

Fortunately, perfect CSI is available at the related PU receiver as a reliable assumption to satisfy SNR for the maximum likelihood detector. Now, the following THEOREM can be formulated.

Slightly similar to [1], the matrix $\tilde{\mathbf{F}}_l(k)$ is defined as $\mathbf{F}_l(k)\mathbf{F}_l(k)^H$ for the l th PU network in the k th sub-carrier.

THEOREM 1: An upper-band of the worst case of the pair-wise error probability as the cost-function is minimized under imperfect CSI at the transmitter for the l th PU network. This can be written as (6):

$$\min_{\substack{\lambda \sim (k) \\ \mathbf{F}_l}} \{WC(g) = - \sum_{k=1}^K \sum_{j=1}^{N_f} \sum_{i=1}^{N_f} \log \{ 1 + \eta \lambda_{\mathbf{R}_{l,P_l P_l}}(k, g)_i \lambda_{\mathbf{T}_{l,P_l P_l}}(k, g)_i \lambda \sim (k)_i \} \}. \quad (6)$$

Proof: see Appendix B.

In (6), g is a parameter related to imperfect CSI at the transmitter. $WC(g)$ refers to the *worst case* of the pair-wise error probability. In the k th sub-carrier for the sub-channel between the l th PU transmitter and the l th PU receiver ($\mathbf{H}_{l,P_l P_l}(k)$), $\lambda_{\mathbf{R}_{l,P_l P_l}}(k, g)_j$ is the j th eigen-value of the receive-eigen-value matrix $\mathbf{\Lambda}_{\mathbf{R}_{l,P_l P_l}}(k, g)$ of the receive-correlation matrix $\mathbf{R}_{l,P_l P_l}(k, g)$. Meanwhile, $\lambda_{\mathbf{T}_{l,P_l P_l}}(k, g)_i$ is the i th eigen-value of the transmit-eigen-value matrix $\mathbf{\Lambda}_{\mathbf{T}_{l,P_l P_l}}(k, g)$ of the transmit-correlation matrix $\mathbf{T}_{l,P_l P_l}(k, g)$. η is a parameter that depends on some factors such as the noise variance and the minimum Euclidean distance metric.

THEOREM 2: When the system is operated in both transmit- and receive-correlation scenarios, the total average interference powers in the underlay scenario for the l th PU network can be written as (7)–(8):

$$Int_1(g) = \sum_{\substack{l=1 \\ l \neq l}}^L \sum_{k=1}^K \sum_{i=1}^{N_f} (\lambda \sim^H(k)_i \lambda_{\mathbf{R}_{l,P_l P_l}}(k, g)_i + \lambda \sim(k)_i \lambda_{\mathbf{T}_{l,P_l P_l}}(k, g)_i), \quad (7)$$

$$Int_2(g) = Q \sum_{l=1}^L \sum_{k=1}^K \sum_{i=1}^{N_f} (n \lambda \sim^H(k)_i \lambda_{\mathbf{R}_{l,S_l P_l}}(k, g)_i). \quad (8)$$

Proof: see Appendix C.

The total average interference powers Int_1 and Int_2 respectively refer to the channels that were declared as (4)–(5). For example, the declared interference by l th PU transmission to the l th PU receiver (Int_1 related to (4)) can be written as (7). g refers to the robust solving.

In (8), $Q > 1$ is an arbitrary gain so that SUs have higher rates.

PROPOSITION 1: Slightly similar to [11- eq.2], P_{Eve} as the probability of eavesdropping can be written as (9):

$$P_{Eve} (\|H_{main}(g)\|_F^2 < \|H_{wire-tap}(g)\|_F^2) = \iint_{x < y} \frac{1}{\partial_{main}^2(g) \partial_{wire-tap}^2(g)} \exp\left(-\frac{x}{\partial_{main}^2(g)} - \frac{y}{\partial_{wire-tap}^2(g)}\right) dx dy = \frac{\partial_{wire-tap}^2(g)}{\partial_{main}^2(g) + \partial_{wire-tap}^2(g)}. \quad (9)$$

More Discussion: see Appendix D.

In (9), ∂_{main}^2 is the gain of the equivalent main channel related to (3). Moreover, $\partial_{wire-tap}^2$ is the gain of the equivalent wire-tap channel (5). This gain is obtained as (8) that should be multiplied by invers of the noise variance. Subsequently, the gain of the equivalent main channel is obtained as (10.3). As discussed in II.A, in this study, secrecy is defined only related to the wire-tap channel (5).

The optimization problem for the l th PU network in order to achieve the optimum JPROC is realized as (10):

$$\min_{\substack{\lambda \sim (k) \\ \mathbf{F}_l \\ k=1, \dots, K \\ l=1, \dots, L}} WC(g)$$

Subject to :

- 1) $P_{Eve}(g) \leq P_{out}$
- 2) $P_{Tot-Int}(g) : Int_1(g) + Int_2(g) \leq I_{Th}$
- 3) $SNR(g) : \frac{1}{\partial_n^2} \sum_{l=1}^L \sum_{k=1}^K \sum_{i=1}^{N_f} n (\lambda \sim(k)_i \lambda_{\mathbf{T}_{l,P_l P_l}}(k, g)_i) \leq P_{R_{sens}}$
- 4) $P_{Tot}(k) : \sum_{i=1}^{N_f} \lambda \sim(k)_i \leq P_{Th}(k), k = 1, \dots, K$
- 5) $\lambda \sim(k)_i \geq 0, k = 1, \dots, K.$

Five constraints for the optimization problem are considered. An outage probability (P_{out}) should be defined for the probability of eavesdropping as the sub-equation (10.1). An interference temperature threshold as the (I_{th}) should be defined for the total average interference powers on the l th PU receiver as the sub-equation (10.2). A threshold ($P_{R_{sens}}$) for the received-power as SNR should be defined in order to have received-power above the *receiver sensitivity* at the detectors as the sub-equation (10.3). A threshold ($P_{Th}(k)$) should be defined for the transmit-

power in the k th sub-carrier as (10.4). Finally, (10.5) indicates that the JPROC matrix is *positive semi-definite*.

The basis of the optimization problem is that the eigenvalues of the JPROC as objective-functions are supposed to be obtained from the received sub-datas at the maximum likelihood detector.

How to obtain (10.3) and (10.4) are given in Appendix E.

THEOREM 3: *The robust optimization problem is convex with constraints (10.1)-(10.5).*

Proof: see Appendix F.

IV. PERFORMANCE CHECKOUT AS CLOSED-FORM SOLUTION

THEROEM 4: $\lambda_{\tilde{F}_l}^*(k)^-$ for the k th sub-carrier and the i th transmit-antenna can be obtained by solving (11):

$$\begin{aligned} \sum_{j=1}^{N_r} \frac{\lambda_{\mathbf{r}_t, P_l P_l}(k, g)_i \lambda_{\mathbf{r}_t, P_l P_l}(k, g)_i}{1 + \lambda_{\mathbf{r}_t, P_l P_l}(k, g)_i \lambda_{\mathbf{r}_t, P_l P_l}(k, g)_i \lambda_{\tilde{F}_l}^*(k)^-} = \\ \rho_1 \{ \text{MAK1}(g, \lambda_{\tilde{F}_l}^*(k)^-) \} + \\ \rho_2 \{ \{ Q \sum_{l=1}^L n \lambda_{\mathbf{r}_t, S_l P_l}(k, g)_i + \sum_{\substack{l=1 \\ l \neq i}}^L \lambda_{\mathbf{r}_t, P_l P_l}(k, g)_i \} \} \\ + \rho_3 \{ \frac{n}{Q^2} \sum_{l=1}^L \lambda_{\mathbf{r}_t, P_l P_l}(k, g)_i \} \\ + \rho_4. \end{aligned} \quad (11)$$

Proof: see Appendix G.

In (11), $x^- = \min \{ \max \{ 0, x \}, \min \{ x, 1 \} \}$. ρ_1, ρ_2, ρ_3 and ρ_4 are respectively the non-negative Lagrange multipliers associated with constraints (10.1)-(10.4). In addition, $\text{MAK1}(g, \lambda_{\tilde{F}_l}^*(k)^-)$ can be written as (12) with respect to derivative operations:

$$\begin{aligned} \text{MAK1}(g, \lambda_{\tilde{F}_l}^*(k)^-) = \\ \frac{-nQ \sum_{l=1}^L \lambda_{\mathbf{r}_t, P_l P_l}(k, g)_i}{\{ \sum_{l=1}^L \lambda_{\tilde{F}_l}^*(k)^- \lambda_{\mathbf{r}_t, P_l P_l}(k, g)_i + nQ \}^2}. \end{aligned} \quad (12)$$

The closed-form solution (11) according to THEOREM 4 and using *dual-Lagrange method* can be easily solved, where $\lambda_{\tilde{F}_l}^*(k)^- = \lambda_{\tilde{F}_l}^{*H}(k)^-$.

V. ANALYTICAL RESULTS

The correlation coefficient between the p th transmit-antenna and the q th receive-antenna for the k th sub-carrier for all the correlation matrices can be attained as [1-Sec. V]: $\zeta J_0(2\pi |p - q| \sin \Omega(k) d / \lambda)$. λ is the wavelength of the carrier. As discussed in [1-Sec. V], $\Omega(k)$ is the angle spread for the k th sub-carrier that should be generated from a uniform distribution in the range $[\bar{\Omega} - \Omega_0 / 2, \bar{\Omega} + \Omega_0 / 2]$.

$\bar{\Omega}$ is the *mean angle spread* that is set to 6° ([1-Sec. V]). d is the spacing between the antennas, J_0 is the zeroth-order Bessel function of the first kind. ζ is the antenna array power gain ([1-Sec. V]).

CVX (or YALMIP) version 2013 ([17]) is used for the optimization problem in the simulations. The total average SNR definition is used. Each data stream is produced as a vector as long as the sub-carriers, i.e., containing 16 sub-datas. Note that half of the sub-carriers are used to achieve the multiplexing gain in all the tests. The number of PUs is set to 3. The number of SUs is set to 1, but not for Fig.10. The total transmit-power in each sub-carrier as $P_{i_{th}}(k)$ is considered 1 Watt. The maximum ratio combining algorithm for the maximum likelihood detector part at the PU receivers is used as [16]. Rayleigh fading channels are generated constantly by the time in each Monte Carlo trial as quasi-static channels. There is no correlation at the receive-sides, i.e., the used receive-angle spreads are large enough and all the receive-correlation matrices are identity. Some other simulation parameters are listed in Table II. Of course, g in Fig. 5 and $Int2$ in Figs. 7 and 8 are varied to show the effects of these parameters.

TABLE II. SOME SIMULATION PARAMETERS

Parameter	Value
Number of sub-carriers (K)	16, [1]
Modulation	BPSK
Antenna Configurations in Down-Link: $N_t \times N_r$	2-by-2
I_{th}	100 m Watt, [1]
g	0
Transmit-Angle Spread	20 Degree, [1]

The complexity of the proposed system in this study compared to [1] are plotted in Fig.4 for the various number of transmit- and receive-antennas and sub-carriers. This is a proportion to find out that the running time in terms of second how much can be affected in the proposed trade-off

scheme compared to [1]. In other words, it is important to find about whether this is implementable or not.

The probability of error is plotted against SNR regime in Fig.5, while the estimation error related to the correlation matrices is varied. As observed, the system performance for the high error estimation g is widely destroyed.

The secrecy capacity is plotted against SNR regime in Fig.6, while Int_2 is varied. The secrecy capacity is decreased by increasing the value of Int_2 . Indeed, the signal to interference-noise ratio is considered in this test.

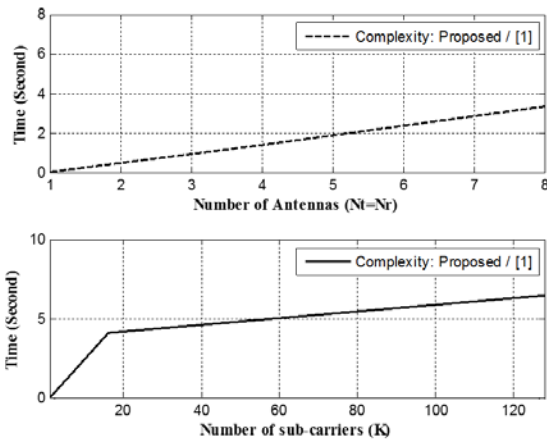


Fig.4. The complexity of the proposed system compared to [1] for the various number of transmit- and receive-antennas and sub-carriers

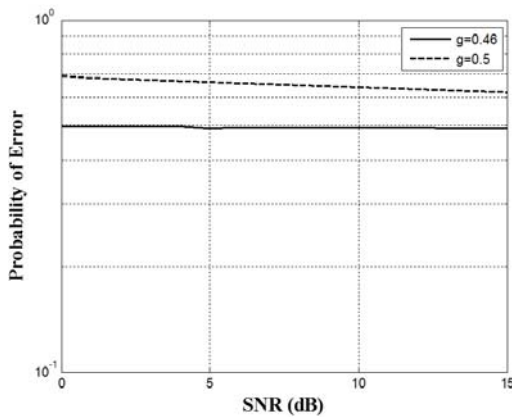


Fig.5. The probability of error versus SNR while changing the value of the estimation error related to the correlation matrices

The probability of eavesdropping is plotted against SNR regime in Fig.7, while Int_2 is varied. The probability of eavesdropping is increased by increasing the value of Int_2 .

The sum of the total average interference powers as (10.2) is plotted against SNR regime in Fig.8, while the transmit-rate of SUs is varied in the underlay scenario. The sum of the total average interference powers is not changed at all, i.e., that is controlled.

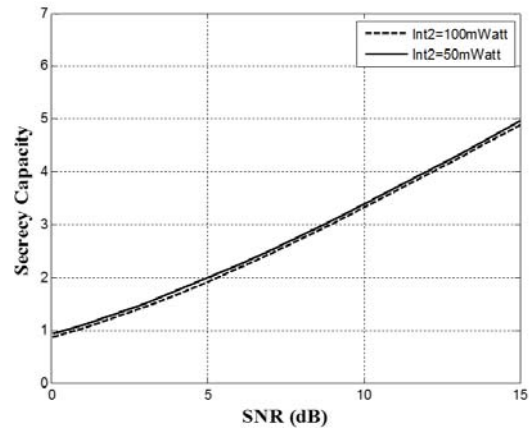


Fig.6. The secrecy capacity versus SNR while changing Int_2

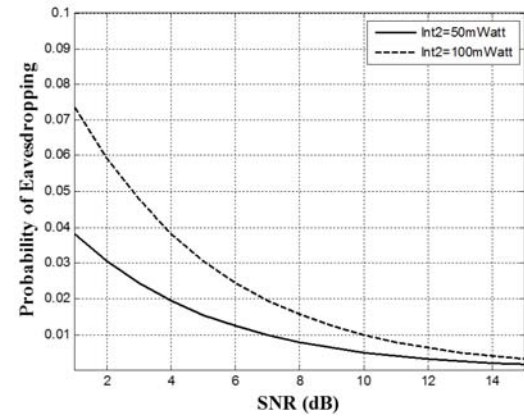


Fig.7. The probability of eavesdropping versus SNR while changing Int_2

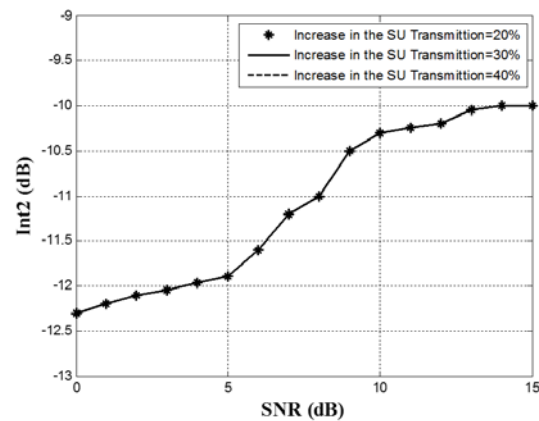


Fig.8. Int_2 versus SNR while changing the transmit-rate of SUs

The probability of error is plotted against SNR regime in Fig.9, while comparing the un-coded system with the coded-system. In this test, the un-coded system has not been JPRO Coded, where only OSTB Coding has been used. As observed, the performance of the system is guaranteed.

The probability of error is plotted against SNR regime in Fig.10, while changing the number of SUs. The probability of error is increased by increasing the number of SUs. In this test, we have 1 PU.

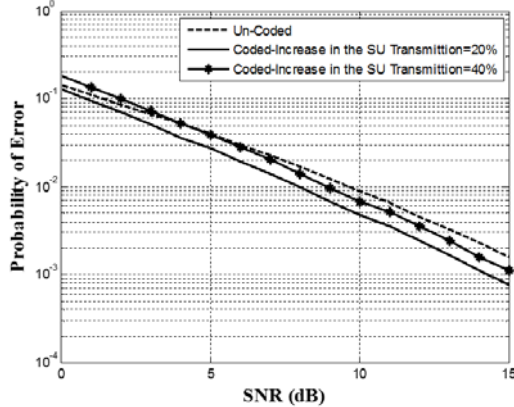


Fig.9. The probability of error versus SNR while comparing the un-coded system with the coded-system

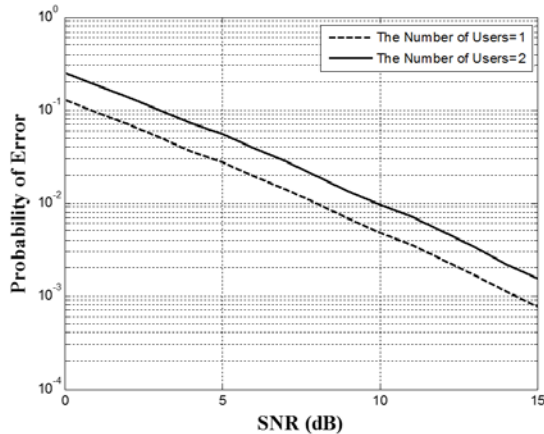


Fig.10. The probability of error versus SNR while changing the number of SUs

VI. CONCLUSION

A design of a JPROC for MIMO OFDM-based cognitive radio systems in the underlay scenario has been discussed. The designed JPROC is established to combat the correlation effects in frequency selective correlated Rayleigh fading channels. This is able to handle the interferences in the underlay scenario on the related PU network in the multi-user scenario. The main contribution is a novel algorithm for the considered systems. We have shown that the main criterion is to establish a controllable trade-off between SU and PU networks, whereas SUs have higher rates. The bad effect on the probability of error in the main PU network is improved by applying OSTFBCs with respect to that channels are frequency selective. The design issue has been totally written as a robust closed-form solution. The problem has been investigated in details and more insights have been provided. The performance of the system has been explored as the probability of error

with respect to the un-desired interferences and the probability of eavesdropping. The study has been supported through presenting the analytic outcomes.

APPENDIX A. HOW TO DETECT SUB-DATAS IN FIG.2

(A-1) is written as above to detect $C_1(k)$. (A-1) is written based on the maximum ratio combining algorithm and with respect to $\mathbf{H}_{i,P_i}(k)$ and (A-2). The mentioned algorithm was used for the maximum likelihood detection in [16]. $\mathbf{H}_{i,P_i}(k)$ is supposed to be estimated by CHEST. Certainly, there is a similar way to estimate $C_2(k)$.

$$\begin{aligned} \hat{C}_1(1) = & \\ & h_1^*(1) \times r_1(1) + h_2(1) \times r_2^*(1) + \\ & h_3^*(1) \times r_3(1) + h_4(1) \times r_4^*(1) + \\ & h_2(2) \times r_1^*(2) + h_1^*(2) \times r_2(2) + \\ & h_4(2) \times r_3^*(2) + h_3^*(2) \times r_4(2), \end{aligned} \quad (\text{A-1})$$

for $2 - by - 2$

equivalent sub-channel matrix:

$$\begin{bmatrix} h_1(1) & h_2(1) \\ h_3(1) & h_4(1) \end{bmatrix} \triangleq \mathbf{F}(1)\mathbf{H}_{i,P_i}(1)\mathbf{F}(1) \quad (\text{A-2})$$

and for $2 - by - 2$

received sub-data matrix:

$$\begin{bmatrix} r_1(1) & r_2(1) \\ r_3(1) & r_4(1) \end{bmatrix} \triangleq \mathbf{Y}(1).$$

APPENDIX B. PROOF OF THEOREM 1

How to generate the correlation matrices was discussed in Section V. $j_0(x)$ can also be written as the *Sinc function* $\sin(x)/x$. With respect to $x \triangleq 2\pi \sin \Omega(k)d/\lambda$ in each sub-carrier, $|p-q|$ is varied for the different transmit- and receive- antennas. For example, consider the 4-by-4 matrix \mathbf{MAK} that is introduced in (B-1):

$$\mathbf{MAK} = \begin{bmatrix} 1 & j_0(x)+\Delta_1 & j_0(2x)+\Delta_2 & j_0(3x)+\Delta_3 \\ j_0(x)+\Delta_1 & 1 & j_0(x)+\Delta_1 & j_0(2x)+\Delta_2 \\ j_0(2x)+\Delta_2 & j_0(x)+\Delta_1 & 1 & j_0(x)+\Delta_1 \\ j_0(3x)+\Delta_3 & j_0(2x)+\Delta_2 & j_0(x)+\Delta_1 & 1 \end{bmatrix} \quad (\text{B-1})$$

With the knowledge of $J_0(2x) = \cos x J_0(x)$ and $J_0(3x) = (\cos^2 x - 1)J_0(x)/3$ on the one hand, and by inserting them in (B-2) and by solving that on the other hand, the mentioned eigen-values $\lambda_{C_i,P_i}(k, \Delta_i)_i^*$ for the k th sub-carrier can be written

as (B-3):

$$\begin{aligned}
 & |\mathbf{MAK} - \lambda \mathbf{I}_4| = 0 \rightarrow (1 - \lambda)^4 - \\
 & 2a^2(1 - \lambda)^2 + 4ba^2(1 - \lambda) - 2b^2(1 - \lambda)^2 \\
 & - a^2(1 - \lambda)^2 + a^4 - 2ca^3 - 2a^2b^2 + 4abc(1 - \lambda) \\
 & + b^4 - 2acb^2 - c^2(1 - \lambda)^2 + a^2c^2 = 0, \\
 & \lambda_{1,2} = 1 + eee_+^{-1}lk, \lambda_{3,4} = 1 - eee_+^{-1}lk, \\
 & lk = a/2 + c/2, \\
 & eee = (5a^2 - 8ab - 2ac + 4b^2 + c^2)^{(1/2)} / 2 \\
 & , a = j_0(x), b = j_0(2x), c = j_0(3x).
 \end{aligned} \tag{B-2}$$

Note that the elements of the example matrix \mathbf{MAK} certainly have error in their estimations as *estimation error* Δ_{i-1} . The subscript \mathbf{C} refers to the correlation matrices. The subscript i refers to the number of eigen-values whose number is 4 in here ($i = 1, 2, 3, 4$). Note that $\Omega(k)$ is the only stochastic process in x . Hence, we can conclude that Δ_i is only in the estimation of the transmit- and the receive- angle spreads.

Let us obviously verify the imperfect CSI at the PU transmitters in this study. The eigen-values of the matrix \mathbf{MAK} are based on Δ_{i-1} as $\lambda_{\mathbf{C}_{i,\rho\eta}}(k, \Delta_{i-1})^*_i$ (under the assumption that each element of \mathbf{MAK} is in the range $[0, 1]$). Now, by defining g as a threshold for $\|\Delta_{i-1}\|$ as $g \leq \|\Delta_{i-1}\|$, the eigen-values of \mathbf{MAK} can be written as $\lambda_{\mathbf{C}_{i,\rho\eta}}(k, g)^*_i$. Note upon CORROLARY 1 that is given as follows.

COROLARY I: The *worst case* of the cost-function as $\max_{\|\Delta_i\| \leq g} WC(\Delta)$ is satisfied, when $\|\Delta_{i-1}\| = g$.

Proof. Let us straightforwardly prove how to convert $\|\Delta_{i-1}\| \leq g$ to $\|\Delta_{i-1}\| = g$. It is obvious that the cost-function experiments its worst case. As discussed in Section I, this refers to have more correlated channels and the minimum of SNR and correspondingly the maximum of the probability of error. For example, consider $\begin{bmatrix} 1 & 0.2 \\ 0.2 & 1 \end{bmatrix}$, instead of \mathbf{I}_2 for the correlation matrices and then, see (6).

Note that we are unable to solve the optimization problem based on Δ , but we are able to do that based on g as a controllable parameter. With the special emphasis on this notation and CORROLARY 1, we can continue.

As previous works, the pair-wise error probability can be defined as:

$$\begin{aligned}
 P_b &= P(\mathbf{C}_i \rightarrow \mathbf{C}_j | \mathbf{H}_{eq,t,\rho\eta P_i}(g)) \leq \\
 & \frac{1}{2} \exp\left(\frac{-1}{2} \|\mathbf{N}^{-1} \mathbf{F}^{-1} \mathbf{F}_i \mathbf{H}_{i,\rho\eta P_i}(g) \mathbf{F}_i (\mathbf{C}_i - \mathbf{C}_j)\|_F^2\right).
 \end{aligned} \tag{B-4}$$

Let us explain the SIRP model. SIRP model is very helpful, when there are so many signals that are supposed to be modeled such as indoor environments or clutter issue, etc. A multi-variant Gaussian process can be modeled as SIRP ([23]). Now, the channels that were introduced in (3)-(5) as arrays of sizes $N_t \times N_r \times K$ can be easily considered as multi-variant Gaussian processes, namely as spherically invariant random vectors whose vectors are sub-channels. For example, (B-5) is written for $\mathbf{H}_{i,\rho\eta P_i}$:

$$\begin{aligned}
 \mathbf{H}_{i,\rho\eta P_i} &= \\
 & [\mathbf{H}_{i,\rho\eta P_i}(0) \mathbf{H}_{i,\rho\eta P_i}(1) \dots \mathbf{H}_{i,\rho\eta P_i}(K)].
 \end{aligned} \tag{B-5}$$

Now, the pair-wise error probability can be obtained as:

$$\begin{aligned}
 P(\mathbf{C}_i(k) \rightarrow \mathbf{C}_j(k) | \mathbf{H}_{i,\rho\eta P_i}(g, k)) &\leq \\
 & \frac{1}{2} \exp\left(\frac{-\chi_{\min}}{4\partial_n^2} \tilde{\mathbf{h}}_{i,\rho\eta P_i}(g, k) (\mathbf{I}_{N_r} \otimes \dots \right. \\
 & \left. \mathbf{F}_i(k) \mathbf{F}_i^H(k) \tilde{\mathbf{h}}_{i,\rho\eta P_i}(g, k)\right).
 \end{aligned} \tag{B-6}$$

The probability density function for $\tilde{\mathbf{h}}_{i,\rho\eta P_i}$ as a vectored SIRP-modeled channel can be written as (B-7). In (B-7), \otimes is the Kronecker product and $\det(\cdot)$ is the determinant operation:

$$\begin{aligned}
 f_h(\tilde{\mathbf{h}}_{i,\rho\eta P_i}(g)) &= \\
 & \left(\frac{1}{\sqrt{2\pi^{KN_r}} \det(\mathbf{R}_{i,\rho\eta P_i}(g) \otimes \mathbf{T}_{i,\rho\eta P_i}(g))} \right) \\
 & \times \exp\left(\frac{-1}{2} \tilde{\mathbf{h}}_{i,\rho\eta P_i}(g) \tilde{\mathbf{h}}_{i,\rho\eta P_i}(g)\right).
 \end{aligned} \tag{B-7}$$

$\mathbf{E} = \mathbf{C}_i - \mathbf{C}_j$ is error in data detection, where $\mathbf{E}\mathbf{E}^H = \chi_{\min} \mathbf{I}_{N_r}$. χ_{\min} is a parameter that depends on some factors such as the noise variance and the minimum Euclidean distance metric.

Using moment generating function for Rayleigh distribution as (B-8):

$$\begin{aligned}
 MGF(s) &= \\
 & |\mathbf{I}_{N_r N_r} - s \frac{\chi_{\min}}{4\partial_n^2} (\mathbf{I}_{N_r} \otimes \mathbf{F}_i(k) \mathbf{F}_i^H(k)) \dots \\
 & (\mathbf{R}_{i,\rho\eta P_i}(g, k) \otimes \mathbf{T}_{i,\rho\eta P_i}(g, k))|^{-1},
 \end{aligned} \tag{B-8}$$

and slightly similar to [1], the upper-band of the average pair-wise error probability can be obtained as:

$$P(\mathbf{C}_i(k) \rightarrow \mathbf{C}_j(k)) \leq \prod_{k=1}^K \left\{ \det \left\{ \mathbf{I}_{N_t N_r} + \frac{\chi_{\min}}{4\partial_n^2} (\mathbf{I}_{N_r} \otimes \mathbf{F}_l(k) \mathbf{F}_l^H(k)) \cdot \cdot \right. \right. \\ \left. \left. (\mathbf{R}_{t, P_t P_t}(g, k) \otimes \mathbf{T}_{t, P_t P_t}(g, k)) \right\}^{-1} \right\}. \quad (\text{B-9})$$

Applying the eigen-value decomposition on the correlation matrices and knowing (B-10) as:

$$(\mathbf{A} \otimes \mathbf{B})(\mathbf{C} \otimes \mathbf{D}) = (\mathbf{AC}) \otimes (\mathbf{BD}), \quad (\text{B-10})$$

and slightly similar to [1], we have (B-11) as:

$$P(\mathbf{C}_i(k) \rightarrow \mathbf{C}_j(k)) \leq \prod_{k=1}^K \left\{ \det \cdot \cdot \cdot \right. \\ \left. \left\{ \mathbf{I}_{N_t N_r} + \frac{\chi_{\min}}{4\partial_n^2} \Lambda_{\mathbf{R}_{t, P_t P_t}}(g, k) \otimes \cdot \cdot \cdot \right. \right. \\ \left. \left. \Lambda^{H/2} \mathbf{T}_{t, P_t P_t}(g, k) \tilde{\mathbf{F}}_l(k) \Lambda^{1/2} \mathbf{T}_{t, P_t P_t}(g, k) \right\}^{-1} \right\}. \quad (\text{B-11})$$

Slightly similar to [1], the upper-band of the average pair-wise error probability can be obtained as:

$$\min_{\lambda \sim (k)} \{ WC(g) = \prod_{k=1}^K \prod_{j=1}^{N_r} \det \{ \cdot \cdot \cdot \} \cdot \cdot \cdot \} \\ \{ \mathbf{I}_{N_t} + \eta \lambda_{\mathbf{R}_{t, P_t P_t}}(k, g)_j \tilde{\mathbf{F}}_l(k) \Lambda_{\mathbf{T}_{t, P_t P_t}}(k, g) \}, \quad (\text{B-12})$$

where $\eta \triangleq \frac{\chi_{\min}}{4\partial_n^2}$. We know that we can minimize the

$\log(Y)$ instead of Y . Besides, we know:

$$\log \left\{ \det \left\{ \begin{bmatrix} a & 0 & \dots & 0 \\ 0 & b & 0 & \dots \\ \dots & 0 & \dots & 0 \\ 0 & \dots & 0 & z \end{bmatrix} \right\} \right\} = a + b + \dots + z. \quad (\text{B-13})$$

Now, $WC(g)$ as an upper-band of the average pair-wise error probability can be robustly obtained as (6).

On the other hand, as discussed in sub-section II.C, half of the sub-carriers are used for spatial multiplexing in this study. It makes that the diversity gain straightforwardly to be multiplied by at most 2 compared to that all of them are used for spatial multiplexing. This refers to the frequency diversity.

APPENDIX C. PROOF OF THEOREM 2

To get the receive-power, the transmit-power should be mathematically multiplied by the square of the equivalent channel norm. With the knowledge of the transmitted data and the equivalent channel and $P_r = P_t \|\mathbf{H}_{eq}\|_F^2$, $Int_1(k)$ can be formulated as (C-1):

$$Int_1(k | \mathbf{C}(k), \mathbf{H}_{t, P_t P_t, eq}(k)) = P_t(k) \times \|\mathbf{H}_{t, P_t P_t, eq}(k)\|_F^2 = \\ Tr \{ \mathbf{F}_l(k) \mathbf{H}_{t, P_t P_t}(k) \mathbf{F}_l(k) \mathbf{C}(k) \mathbf{C}^H(k) \cdot \cdot \cdot \\ \mathbf{F}_l^H(k) \mathbf{H}_{t, P_t P_t}(k) \mathbf{F}_l^H(k) \} \Rightarrow Int_1(k) = E_{\mathbf{H}_{t, P_t P_t}} \{ Tr \{ \cdot \cdot \cdot \} \cdot \cdot \cdot \} \\ \mathbf{H}_{t, P_t P_t}(k) \mathbf{F}_l(k) \mathbf{H}_{t, P_t P_t}(k) \tilde{\mathbf{F}}_l^H(k) \}. \quad (\text{C-1})$$

This equation related to the k th sub-channel is written after applying the symbol $E(\cdot)$ as the expectation operation on the data and the k th sub-channel as the stochastic processes. This is done with the knowledge of the transmitted code $\mathbf{C}(k)$ and the k th equivalent sub-channel ($\mathbf{H}_{eq, t, P_t P_t}(k)$). (C-2) implies the total interference Int_1 :

$$Int_1 = \sum_{k=1}^K Tr \{ \mathbf{T}_{t, P_t P_t}^{1/2}(k) \tilde{\mathbf{F}}_l(k) \mathbf{T}_{t, P_t P_t}^{H/2}(k) \cdot \cdot \cdot \\ E_{\mathbf{H}_{w, t, P_t P_t}} \{ \mathbf{H}_{w, t, P_t P_t}(k) \mathbf{R}^{H/2}_{t, P_t P_t}(k) \cdot \cdot \cdot \\ \tilde{\mathbf{F}}_l^H(k) \mathbf{R}^{1/2}_{t, P_t P_t}(k) \mathbf{H}_{w, t, P_t P_t}(k) \} \}, \quad (\text{C-2})$$

where:

$$\begin{cases} E_{\mathbf{C}} \{ \mathbf{C}(k) \mathbf{C}(k)^H \} = \mathbf{I}_n, \\ Tr(\mathbf{AB}) = Tr(\mathbf{BA}), \\ \tilde{\mathbf{F}}_l(k) \triangleq \tilde{\mathbf{F}}_l(k) \tilde{\mathbf{F}}_l^H(k). \end{cases} \quad (\text{C-3})$$

After that, (C-4) is written based on a fact that has been mentioned in e.g. [24-eqs. 8-9] related to the n -by- n identity matrix \mathbf{I}_n based on the n -by- n antennas:

$$Int_1 = \sum_{k=1}^K Tr \{ \tilde{\mathbf{F}}_l(k) \mathbf{T}_{t, P_t P_t}(k) \} \times Tr \{ \tilde{\mathbf{F}}_l^H(k) \mathbf{R}_{t, P_t P_t}(k) \} \\ \cdot E_{\mathbf{H}_{w, t, P_t P_t}} \{ \mathbf{H}_{w, t, P_t P_t}(k) \mathbf{A}(k) \mathbf{H}_{w, t, P_t P_t}(k) \} = Tr \{ \mathbf{A}(k) \} \mathbf{I}_n, \quad (\text{C-4})$$

LEMMA [1-p. 770]: If $\tilde{\mathbf{F}}_l(k)$ is an optimal solution for the considered optimization problem, $\tilde{\mathbf{F}}_l(k) \mathbf{U}(k)$ is optimal in which $\mathbf{U}(k)$ is a unitary matrix of size $N_t \times N_t$.

Proof: Straightforwardly, this is because when substituting $\tilde{\mathbf{F}}_l(k) \mathbf{U}(k)$ in all the equations in the optimization problem, they remain unchanged, *without loss of optimality*.

Now, (C-5), (C-6) and (C-7) are respectively written, when applying *eigen-value decomposition*, under the definition that $\mathbf{U}_{\tilde{\mathbf{F}}_l}(k) \triangleq \mathbf{U}_{\mathbf{R}_{t, P_t P_t}}(k) = \mathbf{U}_{\mathbf{T}_{t, P_t P_t}}(k)$:

$$\begin{aligned}
 Int_1 &= \sum_{k=1}^K Tr\{\mathbf{U}_{\mathbf{T}_{t,\rho_i\rho_j}}(k)\mathbf{\Lambda}_{\mathbf{F}_i}(k)\mathbf{U}_{\mathbf{T}_{t,\rho_i\rho_j}}^H(k)\}.. \\
 &\mathbf{U}_{\mathbf{T}_{t,\rho_i\rho_j}}(k)\mathbf{\Lambda}_{\mathbf{T}_{t,\rho_i\rho_j}}(k)\mathbf{U}_{\mathbf{T}_{t,\rho_i\rho_j}}^H(k)\}.. \\
 &\times Tr\{\mathbf{U}_{\mathbf{R}_{t,\rho_i\rho_j}}(k)\mathbf{\Lambda}_{\mathbf{F}_i^H}(k)\mathbf{U}_{\mathbf{R}_{t,\rho_i\rho_j}}^H(k)\}.. \\
 &\mathbf{U}_{\mathbf{R}_{t,\rho_i\rho_j}}(k)\mathbf{\Lambda}_{\mathbf{R}_{t,\rho_i\rho_j}}(k)\mathbf{U}_{\mathbf{R}_{t,\rho_i\rho_j}}^H(k)\},
 \end{aligned} \tag{C-5}$$

$$\begin{aligned}
 Int_1 &= \\
 &\sum_{k=1}^K Tr\{\mathbf{\Lambda}_{\mathbf{F}_i}(k)\mathbf{\Lambda}_{\mathbf{T}_{t,\rho_i\rho_j}}(k)\}.. \\
 &Tr\{\mathbf{\Lambda}_{\mathbf{F}_i^H}(k)\mathbf{\Lambda}_{\mathbf{R}_{t,\rho_i\rho_j}}(k)\} = \\
 &\sum_{k=1}^K Tr\{\mathbf{\Lambda}_{\mathbf{F}_i\mathbf{T}_{t,\rho_i\rho_j}}(k) \otimes \mathbf{\Lambda}_{\mathbf{F}_i^H\mathbf{R}_{t,\rho_i\rho_j}}(k)\},
 \end{aligned} \tag{C-6}$$

$$\begin{aligned}
 Int_1 &= \sum_{k=1}^K Tr\{ \dots \\
 &\left[\begin{array}{cccccc}
 \lambda_1(k) & 0 & \dots & \dots & \dots & 0 \\
 0 & \dots & 0 & \dots & \dots & \dots \\
 \dots & 0 & \lambda_{N_t}(k) & 0 & \dots & \dots \\
 \dots & \dots & 0 & \lambda'_1(k) & 0 & \dots \\
 \dots & \dots & \dots & 0 & \dots & 0 \\
 0 & \dots & \dots & \dots & 0 & \lambda'_{N_r}(k)
 \end{array} \right] \}.
 \end{aligned} \tag{C-7}$$

The recent assumption indicates that the transmit- and the receive-angle spreads should be equal for all the channels that were introduced in (3-5). For (C-7), (C-8) should be satisfied:

$$\begin{aligned}
 \lambda_i(k) &\triangleq \lambda_{\mathbf{F}_i}(k)_i \lambda_{\mathbf{T}_{t,\rho_i\rho_j}}(k)_i, \\
 \lambda'_i(k) &\triangleq \lambda_{\mathbf{F}_i^H}(k)_i \lambda_{\mathbf{R}_{t,\rho_i\rho_j}}(k)_i, \\
 &\left\{ \begin{array}{l}
 1) N_t = N_r = n \\
 2) \mathbf{U}_{\mathbf{F}_i}(k) \triangleq \mathbf{U}_{\mathbf{R}_{t,\rho_i\rho_j}}(k) = \mathbf{U}_{\mathbf{T}_{t,\rho_i\rho_j}}(k).
 \end{array} \right.
 \end{aligned} \tag{C-8}$$

It should be noted that, for Int_2 , $Tr\{\mathbf{T}_{t,S_tP_t}(k)\} = n$, because the n-by-n matrix $\mathbf{T}_{t,S_tP_t}(k)$ has only 1 on its diag.

Meanwhile, it is interesting to point out that, for Int_2 , $E_C\{\mathbf{C}(k)\mathbf{C}(k)^H\}$ is set to $Q\mathbf{I}_n$, instead of \mathbf{I}_n , related to SUs. This indicates that SUs are able to have higher rates. Indeed, $Q > 1$ makes SUs to be had higher rates.

APPENDIX D. THE PROBABILITY OF EAVESDROPPING

System capacity for the related wire-tap channel can be defined as:

$$\begin{aligned}
 C_s &= \\
 &\log_2(1 + SNR(g)) - \log_2\left(1 + \frac{Int_2(g)}{\partial_n^2}\right),
 \end{aligned} \tag{D-1}$$

where ∂_n^2 is the noise variance. The probability of eavesdropping as $P(C_s < 0)$ can be written as (D-1). As discussed in II.A, in this study, secrecy is defined related to the wire-tap channel (5). Note that because of the noise term, the post-coder can be neglected with respect to (D-2):

$$\begin{aligned}
 &\|\mathbf{N}(k)^{-1}\mathbf{F}_l(k)^{-1}\mathbf{F}_l(k)\mathbf{H}_{t,S_tP_t}(k)\mathbf{C}(k)\|_F^2 \\
 &= \frac{1}{\partial_n^2} \|\mathbf{H}_{t,S_tP_t}(k)\mathbf{C}(k)\|_F^2.
 \end{aligned} \tag{D-2}$$

As before, the probability of eavesdropping can be extended as (D-3):

$$\partial_{wire-tap}^2(g) = \frac{Q}{\partial_n^2} n^2. \tag{D-3}$$

APPENDIX E. HOW TO OBTAIN (10.3) AND (10.4)

As before, it is very possible to extend the mentioned equations, namely (10.3) and (10.4) with respect to (E-1) and (E-2), respectively:

$$\|\mathbf{N}(k)^{-1}\mathbf{F}_l(k)^{-1}\mathbf{F}_l(k)\mathbf{H}_{t,P_t}(k)\mathbf{F}(k)\mathbf{C}(k)\|_F^2, \tag{E-1}$$

$$\|\mathbf{F}(k)\mathbf{C}(k)\mathbf{C}^H(k)\mathbf{F}^H(k)\|_F^2. \tag{E-2}$$

The inequality in (10.3) is used as smaller and equal as a conventional optimization trick. The post-coder in (10.3) is neglected. Indeed, the post-coder affects on the signals and noise equally.

APPENDIX F. PROOF OF THEOREM 3

As discussed, the optimization problem is represented as a convex problem. Note that all the constraints and the cost function must be convex for convexity as a necessary and sufficient condition. The convexity of the cost function is described as a robust solution. Furthermore, it should be pointed out that as proven in [17-18], “a non-negative weighted sum of convex functions is convex”. On the other hand, there are only scalars as eigen-values (not matrices) in (10). Also, the LOG function is convex [17-18]. Certainly, (F-1) should be satisfied for the LOG function as [17-18] for $0 \leq \theta \leq 1$:

$$f(\theta x + (1-\theta)y) \leq f(\theta x) + f((1-\theta)y). \quad (F-1)$$

The structures of (10.1), (10.2), (10.3) and (10.4) are pretty similar to the non-negative weighted sum of convex functions as *convex combination*. Meanwhile, \leq in the mentioned constraints is put as an optimization trick.

APPENDIX G. PROOF OF THEOREM 4

Using derivatives according to Karush-Kuhn-Tucker condition as $(\delta L / \delta x) = 0, (\delta L / \delta \mu) = 0, (\delta L / \delta v) = 0$, and knowing that the derivative $\log(1+ax)$ is $a/(1+ax)$, the mentioned theorem can be proven. L is the Lagrange function that is defined as (G-1):

$$\begin{aligned} \text{Lagrange}(\lambda_{\tilde{f}_l}^*(k)_i, \rho_1, \rho_2, \rho_3, \rho_4) = & \\ \text{Cost - Function}(\lambda_{\tilde{f}_l}^*(k)_i) & \\ + \rho_1(P_{Eve}(g, \lambda_{\tilde{f}_l}^*(k)_i) - P_{Out}) & \\ + \rho_2(P_{Tot-Int}(g, \lambda_{\tilde{f}_l}^*(k)_i) - I_{th}) & \quad (G-1) \\ + \rho_3(SNR(g, \lambda_{\tilde{f}_l}^*(k)_i) - P_{R_{sens}}) & \\ + \rho_4(P_{Tot}(\lambda_{\tilde{f}_l}^*(k)_i) - P_{Th}(k)). & \end{aligned}$$

REFERENCES

- [1] A. Punctihewa, V. K. Bhargava, C. Despins, "Linear Precoding for Orthogonal Space-Time Block Coded MIMO-OFDM Cognitive Radio," *IEEE Transactions On Communication*, vol. 59, no. 3, March 2011, pp. 767-779.
- [2] E. Bjornson, B. Ottersten, and E. Jorswieck, "On the impact of spatial correlation and precoder design on the performance of MIMO systems with space-time coding," *Proc. ICASSP*, Apr. 2009, pp. 2741-2744.
- [3] A. Hjørungnes and D. Gesbert, "IEEE Precoding of orthogonal space-time block codes in arbitrarily correlated MIMO channels: Iterative and closed-form solutions," *Transactions On Wireless Comm.*, vol. 6, no. 3, Mar. 2007, pp. 1072-1082.
- [4] L. Jacobs, M. Moeneclaey, "Accurate Closed-Form Approximation of BER for OSTBCs with Estimated CSI on Spatially Correlated Rayleigh Fading MIMO Channels," *IEEE Comm Lett*, vol. 17, no. 3, Mar. 2013, pp. 533-536.
- [5] M. H. Islam and Y. C. Liang, "Robust precoding for orthogonal space-time block coded MIMO Cognitive Radio Networks," in *Proc IEEE SPAWC*, Jun. 2009, pp. 86-90.
- [6] Y. Yang, G. Scutari, Peiran Song, P. Palomar, "Robust MIMO Cognitive Radio Systems Under Interference Temperature Constraints" *IEEE Journal on Selected Areas in Comm*, vol. 31, no. 11, Nov. 2013.
- [7] A. Mukherjee, and A. L. Swindlehurst, "Robust beam-forming for security in MIMO wiretap channels with imperfect CSI," *IEEE Trans. Sig. Proc.*, vol. 59, no. 1, Jan. 2011, pp. 351-361.
- [8] L. Zhang, Y.-C. Liang, Y. Xin, and V. Poor, "Robust cognitive Beam-forming with partial channel state information," *IEEE Trans. Wireless Comm.*, vol. 8, no. 8, Aug. 2009, pp. 4143-4153.
- [9] Z. Shu, Y. Qian, and S. Ci, "On physical layer security for cognitive radio networks," *IEEE Net. Mag.*, vol. 27, no. 3, Jun. 2013, pp. 28-33.
- [10] N.S. Ferdinand, D.B. da Costa, A. L. F. de Almeida, M. Latva-aho, "physical Layer Secrecy Performance of TAS Wiretap Channels with Correlated Main and Eavesdropper Channels", *IEEE Trans. Wireless. Lett*, vol. 3, no. 1, Feb. 2014, pp. 86-89.
- [11] Y. Zou, J. Zhu, X. Wang, V. C.M. Leung, "Improving Physical-Layer Security in Wireless Communications Using Diversity Techniques", Available: arXiv: 1405.3725v1 [cs.IT] 15 May2014.
- [12] X. Sun, J. Wang, W. Xu, and C. Zhao, "Performance of secure communications over correlated fading channels," *IEEE Signal Process. Lett*, vol. 19, no. 8, Aug. 2012, pp. 479-482.
- [13] L. Wang, N. Yang, M. ElKashlan, P. L. Yeoh, and J. Yuan, "Physical layer security of maximal ratio combining in two-wave with diffuse power fading channels," *IEEE Trans. Inf. Forensics Security*, vol. 9, no. 2, Feb. 2014, pp. 247-258.
- [14] Luciano L. Mendes, José Marcos C. Brit." MI-SBTVD: A Proposal for the Brazilian Digital Television System SBTVD", *Journal of the Brazilian Computer Society*, Print version ISSN0104-6500, 2009.
- [15] A. Morsali, S. Talebi "On permutation of space-time- frequency block Codings", *IET Commun.*, Vol. 8, Iss.3, 2014, pp. 315-323.
- [16] S. M. Alamouti, "A simple transmitter diversity scheme for wireless communications," *IEEE J. Select. Areas Comm*, vol. 16, Oct.1998, pp. 1451-1458.
- [17] M. Grant, S. Boyd, and Y. Ye, CVX: Matlab Software for Disciplined Convex Programming, ver. 1.1, Nov. 2007. [Online]. Available: www.stanford.edu/~boyd/cvx.
- [18] V. Sharma, I. Wajid, A. B. Gershman, H. Chen, and S. Lambotaran, "Robust downlink beamforming using positive semidefinite covariance constraints," in *Proc. ITG WSA*, pp. 36-41, Feb. 2008.
- [19] N, D.H.N, H. N. Le, T. L. Ngoc, "block-Diagonalization Precoding in a Multiuser Multicell MIMO System: Competition and Coordination", *IEEE Trans. Wireless Comm*, vol. 13, no. 2, Feb. 2014, pp. 968-981.
- [20] Y. Zou, X. Wang, and W. Shen, "Physical-layer security with Multiuser scheduling in cognitive radio networks," *IEEE Trans. Comm.*, vol. 61, no. 12, Dec. 2013, pp. 5103-5113.
- [21] G. Geraci, M. Egan, J. Yuan, A. Razi, and I. Collings, "Secrecy sumrates for multi-user MIMO regularized channel inversion precoding," *IEEE Trans. Comm.*, vol. 60, no. 11, Nov. 2012, pp. 3472-3482.
- [22] M. K. Simon and M. S. Alouini, "Digital Communication over Fading Channels," *2ed. New York: Wiley, 2005*.
- [23] M. M. Weiner, "Adaptive Antennas and Receivers," *2ed. New York: CRC Press, 2005*.
- [24] M. Ding, S. D. Blostein, "MIMO Minimum Total MSE Transceiver Design with Imperfect CSI at Both Ends", *IEEE Trans. Sig. Proc.*, vol. 57, no. 3, March. 2009, pp. 1141-1150.